Biochemical and Biophysical Research Communications 451 (2014) 367–373

Contents lists available at ScienceDirect

Biochemical and Biophysical Research Communications

journal homepage: www.elsevier.com/locate/ybbrc

ER stress responses in the absence of apoptosome: A comparative study in CASP9 proficient vs deficient mouse embryonic fibroblasts

Shane Deegan [a,b], Svetlana Saveljeva [a,b], Sanjeev Gupta [a,c], David C MacDonald [a,b], Afshin Samali [a,b,*]

[a] Apoptosis Research Centre, NUI Galway, Ireland
[b] School of Natural Sciences, NUI Galway, Ireland
[c] School of Medicine, NUI Galway, Ireland

ARTICLE INFO

Article history:
Received 19 July 2014
Available online 30 July 2014

Keywords:
Endoplasmic reticulum (ER) stress
Apoptosis
Autophagy
Unfolded protein response (UPR)
Caspase

ABSTRACT

Cells respond to endoplasmic reticulum (ER) stress through the unfolded protein response (UPR), autophagy and cell death. In this study we utilized *casp9*$^{+/+}$ and *casp9*$^{-/-}$ MEFs to determine the effect of inhibition of mitochondrial apoptosis pathway on ER stress-induced-cell death, UPR and autophagy. We observed prolonged activation of UPR and autophagy in *casp9*$^{-/-}$ cells as compared with *casp9*$^{+/+}$ MEFs, which displayed transient activation of both pathways. Furthermore we showed that while *casp9*$^{-/-}$ MEFs were resistant to ER stress, prolonged exposure led to the activation of a non-canonical, caspase-mediated mode of cell death.

1. Introduction

The endoplasmic reticulum (ER) is the site for synthesis, folding and maturation of most secreted and transmembrane proteins [1]. The processing of nascent proteins in the ER lumen requires an array of chaperones and folding enzymes that depend on the ER's rich oxidative environment and calcium pools for optimal functioning [2,3]. Physiological or pathological processes that disturb this unique environment cripple the ER's protein folding machinery, a condition referred to as ER stress. Cellular responses to ER stress include the unfolded protein response (UPR), autophagy and apoptosis [4–7].

The UPR is regulated by three ER transmembrane proteins; PKR-like ER kinase (PERK or EIF2AK3), activating transcription factor 6 (ATF6) and Inositol-requiring enzyme 1 (IRE1 or ERN1) [6,8]. The UPR promotes cell survival by attenuating general protein synthesis and restoring cellular homeostasis via the activation of a cascade of transcription factors which upregulate genes encoding (1) chaperones and folding enzymes (2) components of the ER associated degradation (ERAD) machinery and (3) the autophagy machinery [9–11].

Autophagy is an evolutionary conserved bulk degradation pathway that utilizes the lysosome to degrade its substrates [12–14]. Autophagy is upregulated in response to most cellular stresses; including starvation, hypoxia, heat shock, microbial infection and ER stress [7]. During cellular stress large quantities of proteins and organelles are damaged and if they are not removed from the cell they may become toxic, resulting in cell death.

Chronic or acute ER stress will result in the activation of the intrinsic apoptotic pathway [15,16]. Apoptosis is a caspase-dependent form of cell death [17]. The Intrinsic apoptotic pathway requires mitochondrial outer membrane permeabilization (MOMP) leading to cytochrome *c* release from the mitochondria, facilitating the assembly of the apoptosome complex which recruits and sequentially activates CASP9 and CASP3. As such CASP9 is regarded as the initial caspase in the intrinsic mitochondrial pathway. CASP3 is the main downstream effector caspase that cleaves the majority of the cellular substrates in apoptotic cells. Cells from *casp9*-null mice show resistance to apoptosis induced by a range of cytotoxic drugs and irradiation [18,19].

Here, we carry out a comparative study of ER stress responses in CASP9 proficient (*casp9*$^{+/+}$) and CASP9 deficient (*casp9*$^{-/-}$) mouse embryonic fibroblasts (MEFs). We observed differential effect of chronic ER stress on cell morphology, the kinetics of the unfolded protein response, autophagy and cell death.

Abbreviations: ATG, autophagy related; DDIT3, DNA-damage inducible-transcript 3; DNA, deoxyribonucleic acid; DTT, dithiothreitol; ER, endoplasmic reticulum; FADD, fas-associated protein with death domain; GAPDH, glyceraldehyde 3-phosphate dehydrogenase; HSPA5, heat shock 70 kDa protein 5; LC3, microtubule-associated protein 1 light chain 3; MEF, mouse embryonic fibroblasts; MOMP, mitochondrial outer membrane permeabilization; PARP, poly (ADP-ribose) polymerase; PBS, phosphate buffered saline; PI, propidium iodide; Tg, thapsigargin; Tm, tunicamycin; XBP-1, X-box binding protein-1.

* Corresponding author at: Apoptosis Research Centre, NUI Galway, Ireland. Fax: +353 91494596.
E-mail address: afshin.samali@nuigalway.ie (A. Samali).

http://dx.doi.org/10.1016/j.bbrc.2014.07.111
0006-291X/

2. Materials and methods

2.1. Cell culture and treatments

CASP9$^{-/-}$ (*casp9*$^{-/-}$) and matched CASP9$^{+/+}$ (*casp9*$^{+/+}$) mouse embryonic fibroblasts (MEFs) were a kind gift from Prof. Tak Mak, University of Alberta, Canada. MEFs were cultured in Dulbecco's modified Eagle's medium (Sigma–Aldrich, D6429) supplemented with 10% fetal bovine serum (Sigma–Aldrich, F7524), 100 U/ml penicillin and 100 mg/ml streptomycin (Sigma–Aldrich, P0781), L-glutamine (Sigma–Aldrich, G7513), non-essential amino acids (Sigma–Aldrich, M7145) and sodium pyruvate (Sigma–Aldrich, S8636) at 37 °C, 5% CO_2 in a humidified incubator. To induce ER stress, cells were seeded at the required density 24 h prior to treatment, the medium was then removed and replaced with medium containing 0.5 μM of thapsigargin (Sigma–Aldrich, T9033), a SERCA pump inhibitor, or 0.5 μg/mL of tunicamycin (Sigma–Aldrich, T7765), an inhibitor of N-glycosylation.

2.2. Bright field microscopy

Casp9$^{+/+}$ and *casp9*$^{-/-}$ MEFs were treated with either Tg or Tm for the indicated time point. Before imaging cells were fixed using 10% formalin. Images of the cells were taken in bright field using Olympus microscope at 20× magnification.

2.3. Transmission electron microscopy

casp9$^{+/+}$ and *casp9*$^{-/-}$ MEFs were treated with Tg for the indicated time points. Cells were fixed using 2% glutaraldehyde for 1 h. Cells were washed for 3 × 5 min in phosphate buffered saline (PBS) followed by secondary fixation in a buffer of 1% Osmium tetraoxide for 1 h. Cells were then dehydrated by sequential washes in 25% ethanol (10 min), 50% ethanol (10 min) 70% ethanol (10 min) 90% ethanol (10 min) 100% ethanol (10 min). Cells were embedded in 50% resin for 1 h followed by 100% resin for 1 h. Polymerization was carried out at 70 °C for 8 h.

2.4. RNA extraction, RT-PCR and real time PCR

Total RNA was isolated using Trizol (Invitrogen) according to the manufacturer's instructions. Reverse transcription (RT) was carried out with 2 μg RNA and Oligo dT (Invitrogen) using 20 U Superscript II Reverse Transcriptase (Invitrogen). For real-time PCR the cDNA was diluted 1:5 ratio. Probes for EDEM1 (Mm00 551797_m1), PDIA4 (Mm00437958_m1), ATF4 (Mm012986 04_g1), HERPUD1 (Mm01249592_m1), DDIT3 (Mm004920 97_m1), DNAJC3 (Mm00515299_m1) and GAPDH (Mm999999 15_g1) were purchased from Applied Biosystems.

2.5. Western blotting

Cells were washed once in ice-cold PBS and lyzed in whole cell lysis buffer (20 mM HEPES pH 7.5, 350 mM NaCl, 0.5 mM EDTA, 1 mM $MgCl_2$, 0.1 mM EGTA, 1% Triton X-100, protease inhibitor cocktail tablet (Roche, 11836170001) and 10 mM NaF) after the indicated times of treatment and boiled at 95 °C with Laemmli's SDS–PAGE sample buffer for 5 min. Protein concentration was determined by BCA protein assay kit (Thermo Scientific, 23227). Equal amounts (20 μg/lane) of protein samples were run on an SDS polyacrylamide gel. The proteins were transferred onto nitrocellulose membrane and blocked with 5% non-fat milk in PBS containing 0.1% Tween-20 (Sigma–Aldrich, P5927). The membranes were incubated with the primary antibody Anti-LC3-B (Sigma, L7543), CASP9 (Cell Signaling Technology, 9508), CASP3 (Cell Signaling Technology 9664), PARP (Cell Signaling Technology, 9542), DDIT3 (Santa Cruz, sc-793), XBP1s (Biolegend, 619502), EIF2S1 (Cell Signaling Technology, 9722), P-EIF2S1 (Cell Signaling Technology, 9721S) or β-Actin (Sigma–Aldrich, A-5060) for 2 h at room temperature or overnight at 4 °C. All the secondary antibodies were purchased from Jackson. Membranes were developed using Western Lightning ECL substrates (Perkin Elmer, NEL102001EA).

2.6. Annexin V and propidium iodide staining

Externalization of phosphatidylserine (PS) to the outer leaflet of the plasma membrane of apoptotic cells was assessed using Annexin V-FITC as described previously [20]. Briefly, cells were collected by centrifugation at 350*g*, resuspended in ice-cold calcium buffer (10 mM HEPES/NaOH, pH 7.4, 140 mM NaCl, 2.5 mM $CaCl_2$), containing Annexin V-FITC and incubated in the dark for 15 min on ice. Prior to analysis 300 μl of ice-cold calcium buffer containing 4 μl of PI (50 μg/ml) was added immediately before analysis, which was performed using FACS Calibur flow cytometer (Becton Dickinson).

2.7. Statistical analysis

qRT-PCR data is expressed as mean ± SEM for three independent experiments. Differences between the treatment groups were assessed using graph pad's Two-tailed unpaired student's *t*-tests. The values with $p < 0.05$ is considered statistically significant and values with $p < 0.005$ is considered statistically very significant.

3. Results

3.1. Analysis of cell morphology in response to ER stress

It is well established that prolonged ER stress will result in mitochondria-mediated apoptosis (MMA) via activation of the apoptosome [15,21]; however, although studies show CASP9 is required for ER stress-induced apoptosis, no studies have assessed the effect of CASP9 deficiency on the regulation of the UPR and autophagy in response to ER stress. In this study we monitor the effect of CASP9 deficiency on ER stress regulation of UPR, autophagy and cell death.

We first looked at the effects of ER stress on cell morphology through the use of transmission electron microscopy (TEM) and conventional bright phase imaging. TEM was performed on *casp9*$^{+/+}$ and *casp9*$^{-/-}$ cells following 0, 6 and 24 h of Tg treatment. Within the first 24 h of treatment, *casp9*$^{+/+}$ cells showed characteristic morphology associated with apoptosis such as membrane blebbing and nuclear condensation, while *casp9*$^{-/-}$ MEFs showed no morphological features of apoptosis (Fig. 1A). Interestingly, some notable morphological changes were evident in *casp9*$^{-/-}$ MEFs which displayed large vacuoles, indicative of an expansion of the ER membrane at 24 h, indicated with arrows in Fig. 1A. Using bright phase imaging, further assessment of the cells was carried out following 72 h treatment with Tg and Tm. Complete cell death was observed in *casp9*$^{+/+}$ MEFs at 72 h with features indicative of apoptosis. In contrast, *casp9*$^{-/-}$ MEFs were resistant to cell death, although cellular stress was clearly evident at 72 h, showing extensive expansion of ER membrane.

3.2. CASP9 deficient MEFs undergo a delayed ER stress-induced cell death and display activation of effector caspases

Prolonged ER stress can result in the activation of the intrinsic apoptotic pathway, a form of cell death that is mediated through the permeabilization of the mitochondrial membrane and the for-

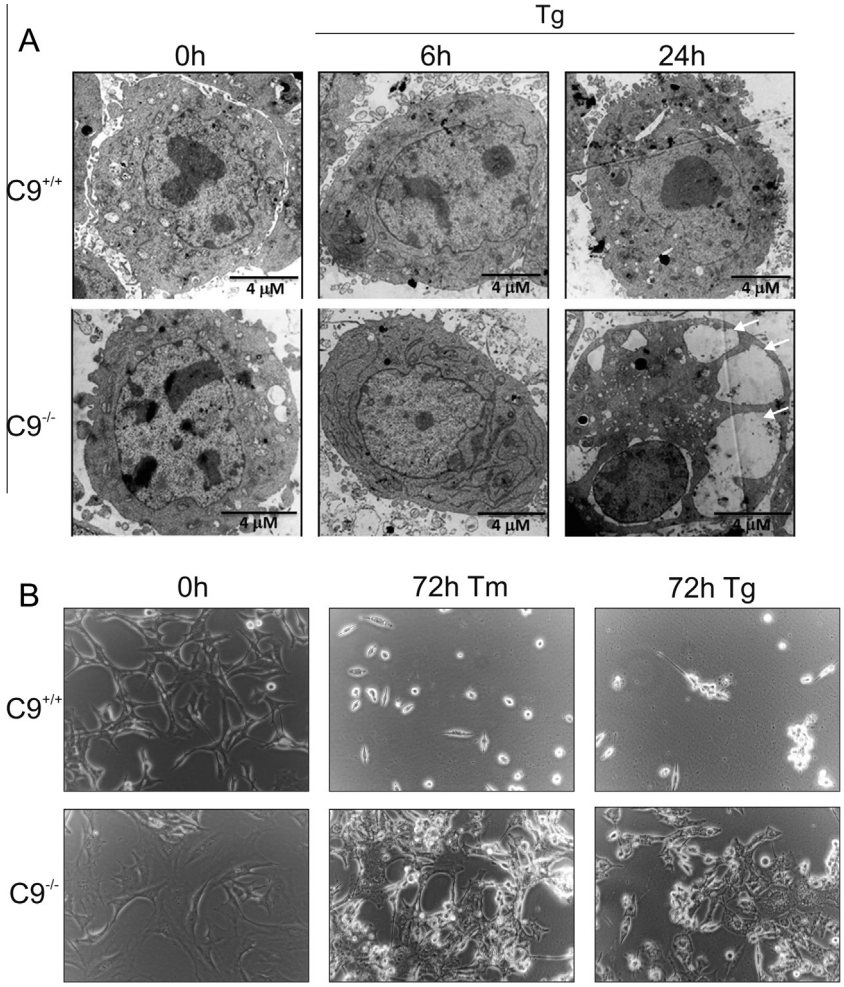

Fig. 1. Loss of CASP9 provides resistance to ER stress-induced apoptosis. (A) *casp9*$^{+/+}$ and *casp9*$^{-/-}$ MEFs were treated with 0.5 μM Tg for 6 h and 24 h and subjected to electron microscopy after fixing. (B) *casp9*$^{+/+}$ and *casp9*$^{-/-}$ MEFs were treated with 0.5 μM Tg or 0.5 μg/ml Tm for 72 h and assessed by bright field microscopy.

mation of the apoptosome complex [22]. To determine the sensitivity of *casp9*$^{+/+}$ and *casp9*$^{-/-}$ MEFs to ER stress-induced cell death we carried out Annexin-V and propidium iodide (PI) double staining to assess both apoptotic and total cell death. Cells were also treated with Hydrogen peroxide (H_2O_2) for 1 h as a positive control for necrotic cell death. Consistent with previous reports [15,21], we observed a robust and significant Annexin-V and PI staining in *casp9*$^{+/+}$ MEFs in the first 24 h of treatment, but not in *casp9*$^{-/-}$ MEFs (Fig. 2A and B). Although *casp9*$^{-/-}$ MEFs did not show a robust increase in Annexin-V and PI staining at 24 h, later time points (48 and 72 h) confirmed that *casp9*$^{-/-}$ cells did indeed undergo cell death being positive for both Annexin-V and PI staining. Analysis of both *casp9*$^{+/+}$ and *casp9*$^{-/-}$ MEFs showed a similar distribution on the dot blots upon treatment; however the kinetics of apoptosis induction in the *casp9*$^{-/-}$ MEFs was slower. The scatter plots clearly show that the *casp9*$^{-/-}$ MEFs are undergoing an apoptotic mode of cell death and we confirmed the activation of the executioner CASP3 using Western blot (Fig. 2C). We confirm here that although *casp9*$^{-/-}$ MEFs are resistant to ER stress, prolonged exposure to the treatment will result in the activation of the executioner CASP3 and subsequent death, suggesting a non-canonical cell death pathway is activated.

3.3. CASP9 deficient cells display a prolonged UPR response

It is well established that prolonged ER stress will result in permeabilization of the mitochondrial outer membrane subsequently releasing cytochrome *c*, driving the formation of the apoptosome [21]; however, no studies have monitored the UPR when this route of cell death is compromised. Here we monitor the effect of CASP9 deficiency on the regulation of UPR. To test whether CASP9 deficiency resulted in a differential UPR we treated *casp9*$^{+/+}$ and *casp9*$^{-/-}$ MEFs with the ER stress inducing agents Tg or Tm, and monitored an array of UPR target genes, both at the RNA level by real-time PCR (Fig. 3B) and at the protein level by immunoblotting (Fig. 3A).

In order to obtain a direct read out of UPR signaling kinetics in *casp9*$^{+/+}$ and *casp9*$^{-/-}$ MEFs we monitored an array of UPR target genes (EDEM1, PDIA4, ATF4, DDIT3, HERPUD1 and DNAJC3) using real-time PCR (Fig. 3B). Basal transcript pools in *casp9*$^{+/+}$ and *casp9*$^{-/-}$ MEFs showed no significant differences; however, upon Tg or Tm treatment, *casp9*$^{+/+}$ MEFs showed an increase of transcript pools over the first 12 h followed by a decline over the course of 12–24 h. In contrast, *casp9*$^{-/-}$ MEF transcript levels increased more gradually and levels were elevated up to 24 h.

To determine whether differences in the kinetics of the response observed at the RNA level were also observed at the protein level we carried out immunoblotting with a cohort of established markers, indicative of the UPR, including DDIT3 (CHOP), total and phosphorylated eIF2α (EIF2S1) and spliced XBP1 (XBP1s) (Fig. 3A). Interestingly, there was no attenuation of EIF2S1 phosphorylation in the *casp9*$^{-/-}$ MEFs upon Tg treatment throughout the 72 h timecourse, and only a negligible decrease at 72 h upon Tm treatment. This also correlated with prolonged

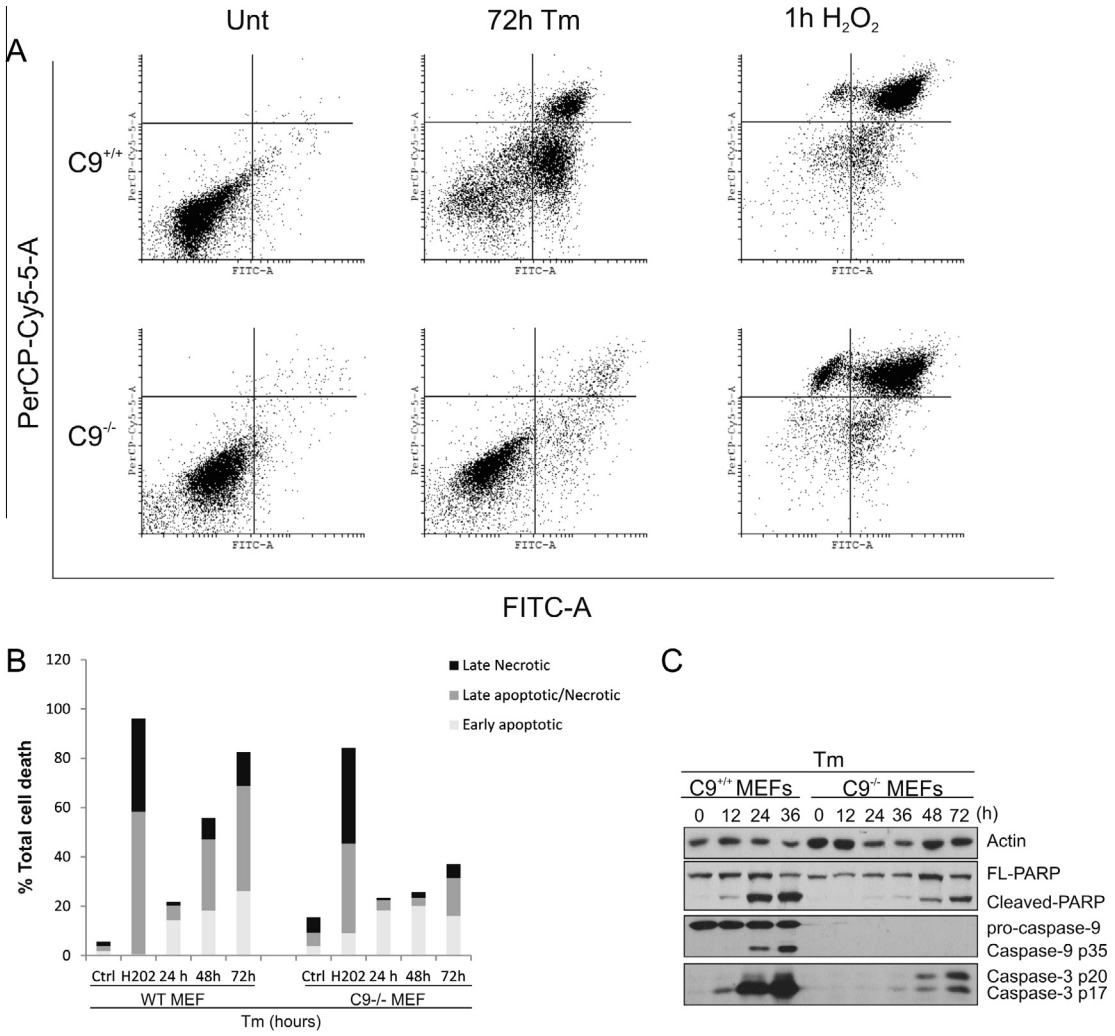

Fig. 2. Casp9$^{-/-}$ MEFs undergo a delayed caspase-mediated cell death. *Casp9*$^{+/+}$ and *casp9*$^{-/-}$ MEFs were treated with 0.5 μg/ml Tm for the indicated time points. (A) Cells were co-stained with Annexin-V as a marker for externalization of phosphatidylserine, indicative of apoptosis and propidium iodide (PI) as an indicator of total cell death. Following co-staining of the cells FACS analysis was carried out. As a positive control for necrotic cell death, cells were treated with H_2O_2 for 1 h. (B) Following a 24, 48 and 72 h time course, cells were co-stained with Annexin-V and Propidium iodide (PI). As a positive control for necrotic cell death, cells were treated with H_2O_2 for 1 h. Following co-staining of the cells FACS analysis was carried out. The percentage of Annexin-V, PI or PI/Annexin-V stained cells was extracted from the dot plots and presented in bar chart format. Average of 3 independent experiments is shown. (C) Immunoblotting of whole cell lysates was performed using antibodies against CASP9, CASP3, PARP and Actin.

expression of DDIT3, a downstream transcription factor of the PERK arm of the UPR signaling. Spliced XBP1 also exhibited a prolonged activation similar to that of DDIT3 and EIF2S1 In contrast, *casp9*$^{+/+}$ MEFs showed early attenuation of EIF2S1 phosphorylation and DDIT3 expression. Studies have shown that prolonged phosphorylation of EIF2S1 protects cells during ER stress-induced cell death which suggests that EIF2S1 dephosphorylation may act as a determining factor for the switch between protective and pro-death UPR signaling [23]. Our results suggest that inhibition of CASP9 may result in prolonged EIF2S1 phosphorylation as well as an overall prolonged UPR response.

3.4. CASP9 deficient cells display prolonged activation of autophagy

To demonstrate that autophagy was induced in *casp9*$^{+/+}$ and *casp9*$^{-/-}$ MEFs in response to ER stress, cells were treated with Tm or Tg with or without chloroquine (CQ). Cells were harvested at the indicated time points and whole cell lysates were assessed by immunoblotting for LC3-I and LC3-II, a marker of autophagosome biogenesis (Fig. 4A). Treatment with CQ inhibits the final degradation step of the autophagosome at the lysosome; thus, if Tm or Tg induces autophagosome biogenesis then inhibition of lysosomal degradation using CQ in combination with treatment should result in enhanced levels of autophagosomes in the cell. We could observe a clear enhancement in LC3-I to LC3-II processing when comparing samples co-treated with CQ, indicating functional autophagic flux.

Using TEM we observed cytosolic dense double membrane vacuoles in *casp9*$^{+/+}$ and *casp9*$^{-/-}$ MEFs in response to Tm treatment. The autophagosomes contained mitochondrial shaped structures as well as other unidentifiable substrates, most likely protein aggregates and damaged organelles (Fig. 4B).

Our results confirm that autophagy is functional in both *casp9*$^{+/+}$ and *casp9*$^{-/-}$ MEFs and is capable of engulfing large cytosolic substrates, confirming the role for autophagy in response to cellular stress. Interestingly, like the kinetics of the UPR, the activation of the autophagy pathway (conversion of LC3I to LC3II) was transient in the *casp9*$^{+/+}$ MEFs but more prolonged in the *casp9*$^{-/-}$ MEFs. It has been widely reported that caspases can cleave components of the autophagy pathway such as ATG3 [24] and BECN1 [25], in turn acting as a feedback mechanism to shut down the pro-survival effects of the autophagy pathway. In contrast to the *casp9*$^{+/+}$ MEFs,

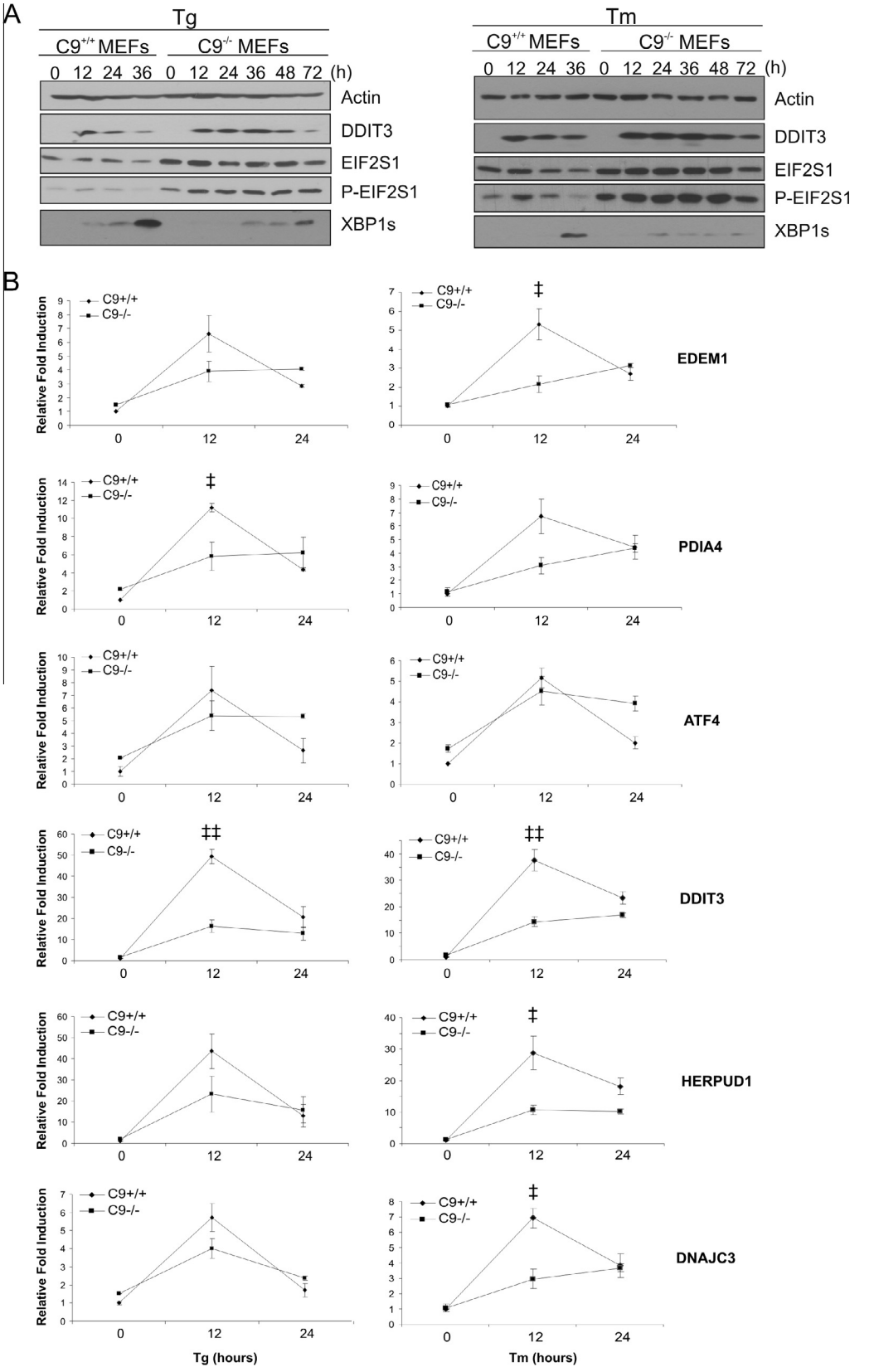

Fig. 3. Differential UPR response in casp9$^{+/+}$ and casp9$^{-/-}$ MEFs. *casp9*$^{+/+}$ and *casp9*$^{-/-}$ MEFs were treated with 0.5 μM Tg or 0.5 μg/ml Tm for the indicated time points. (A) Immunoblotting of total protein was performed using antibodies against Actin, DDIT3, EIF2S1, phosphorylated EIF2S1 (P-EIF2S1) and spliced XBP1 (XBP1s). (B) *casp9*$^{+/+}$ and *casp9*$^{-/-}$ MEFs were harvested in TRIzol at indicated time points. RNA was extracted following manufactures guidelines. 2 μg of RNA was reverse transcribed and the cDNA was diluted in ddH_2O to 1:5 ratio. Real time PCR was carried out on the cDNA using Taqman probes for EDEM1, PDIA4, ATF4, DDIT3, HERPUD1, DNAJC3. Graphs were plotted as relative fold induction in respect to *casp9*$^{+/+}$ 0 h (‡ indicates *p*-value <0.05, ‡‡ indicates *p*-value <0.005).

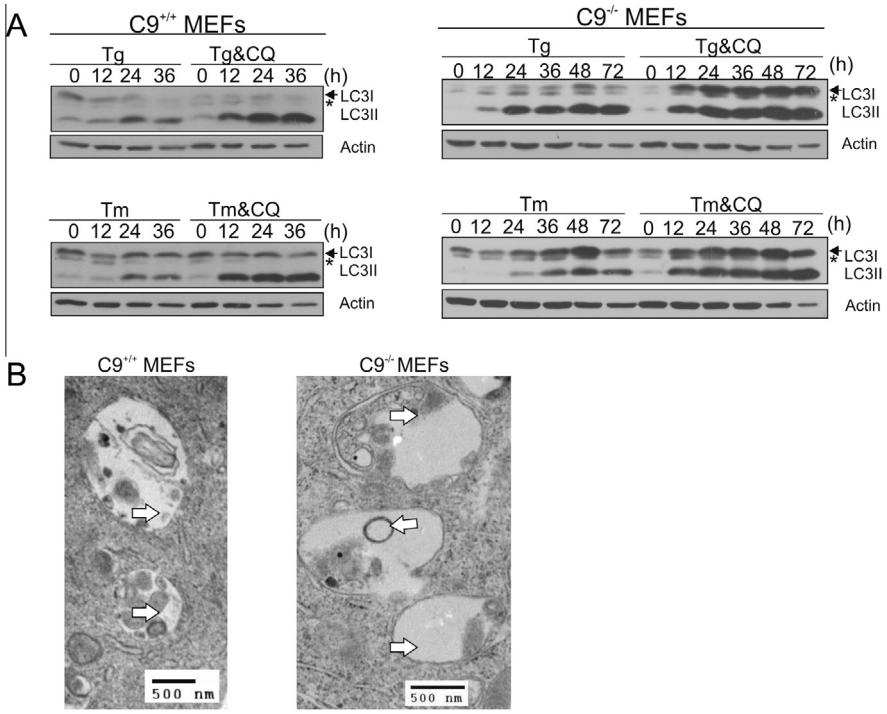

Fig. 4. Monitoring autophagy kinetics in *casp9*$^{+/+}$ and *casp9*$^{-/-}$ MEFs in response to ER stress. (A) *casp9*$^{+/+}$ and *casp9*$^{-/-}$ MEFs were treated with 0.5 μM Tg or 0.5 μg/ml Tm, in the presence or absence of 60 μM of chloroquine to monitor the autophagy flux at indicated time points. Immunoblotting was performed using antibodies against total LC3 and Actin. (B) *casp9*$^{+/+}$ and *casp9*$^{-/-}$ MEFs were treated with 0.5 μM Tg for 24 h and subjected to electron microscopy after fixing. A representative morphology of autophagic vacuoles is shown. (* indicates non-specific band.)

the *casp9*$^{-/-}$ MEFs displayed a continuous activation of autophagy up to 72 h, in a similar manner to the kinetics displayed by the UPR.

4. Discussion

In this comparative analysis of *casp9*$^{+/+}$ and *casp9*$^{-/-}$ MEFs we show that in a wild-type background, ER stress transiently activates both the UPR and autophagy as a survival response to reduce the protein load in the ER and remove any damaged or unwanted substrates that accumulate in response to the stress. Upon activation of CASP9 and subsequently CASP3, both the UPR and autophagy are attenuated and apoptotic cell death ensures. The *casp9*$^{-/-}$ MEFs showed clear resistance to cell death in the initial 24 to 48 h of stress; however, TEM and bright phase images clearly show that the cells were exhibiting clear signs of stress, displaying large vacuole formation, indicative of expanded ER membrane. Later time points, revealed *casp9*$^{-/-}$ MEFs eventually succumbed to cell death. Our laboratory recently characterized the mode of cell death to be mediated by a novel complex consisting of ATG5, FADD and CASP8. The study shows that although MOMP was observed in the *casp9*$^{-/-}$ MEFs we confirmed in BAX/BAK MEFs that the formation of the complex was independent of MOMP. Interestingly, inhibition of ATG5 or ATG7 prevented the processing of CASP8 and CASP3, enhancing cell survival (Deegan et al., *Autophagy* – in press). Furthermore, *casp9*$^{-/-}$ MEFs revealed continuous activation of both the UPR and autophagy in contrast to the *casp9*$^{+/+}$ MEFs which displayed a transient activation of these pathways. Interestingly, in the *casp9*$^{+/+}$ MEFs the deactivation of the UPR and autophagy pathways coincided with the activation of the executioner CASP3. Caspase cleavage of autophagy machinery proteins has been documented previously and it has been suggested that this is a feedback mechanism built into the cell to shut down the survival responses when apoptosis has been initiated [24,25]. Our laboratory have previously shown that inhibition of autophagy via ATG5 knockdown increased the rate of cell death in *casp9*$^{+/+}$ MEFs, confirming autophagy to be a pro-survival response in that model (Deegan et al., *Autophagy* – in press). A similar feedback mechanism to shut down the UPR may also exist upon activation of caspases as a mechanism to enhance cell death. This study clearly reveals the importance of the intrinsic apoptotic pathway for the execution of ER stress-induced cell death; however it also highlights the flexibility of the cell to adapt and find alternative pathways to execute death. Interestingly, our data suggest that caspase activation enhances cell death by shutting down the UPR and autophagy pathways. It has been reported previously that caspases can cleave components of the autophagy machinery such as ATG3 and BECN1; however there have been no reports suggesting caspases can cleave regulators of the UPR. As previously mentioned phosphorylation of EIF2S1 is an essential pro-survival response during ER stress, thus the cell may have a fail-safe mechanism in place to shut down survival responses such as this when the stress becomes too severe.

Understanding how the cell death and cell survival machineries orchestrate their activities and cross-talk to determine cell fate is of fundamental importance. This is important not only under physiological and pathological stress conditions, but also under conditions where induction of death is the desired outcome under stress conditions (e.g., tumor microenvironment).

Conflict of interest

A.S. is a co-founder and director of Aquila Bioscience Ltd.

Financial disclosure statement

This publication has emanated from research conducted with the financial support of Science Foundation Ireland under Grant

Nos. 06/RFP/BIC002 and 05/IN3/B851, Health Research Board (Grant No. HRA_HSR/2010/24) and by Belgian grant – Interuniversity Attraction Poles, IAP 7/32. S.G. work is supported by Health Research Board (Grant No. HRA_HSR/2010/24). S.D. was supported by a fellowship from the College of Science at NUIG.

Acknowledgments

We would like to thank all the members of Apoptosis Research Centre (ARC), at NUI Galway. In particular Dr Sandra Healy for critical reading and feedback on this work. We are grateful to Prof. Tak Mak from the University of Alberta, Canada, for providing the casp9$^{+/+}$ and casp9$^{-/-}$ MEFs.

References

[1] S. Healy et al., Biology of the endoplasmic reticulum, in: P. Agostinis, S. Afshin (Eds.), Endoplasmic Reticulum Stress in Health and Disease, Springer, Netherlands, 2012, pp. 3–22.
[2] Y. Ma, L.M. Hendershot, ER chaperone functions during normal and stress conditions, J. Chem. Neuroanat. 28 (1–2) (2004) 51–65.
[3] B.P. Tu, J.S. Weissman, Oxidative protein folding in eukaryotes: mechanisms and consequences, J. Cell Biol. 164 (3) (2004) 341–346.
[4] D. Ron, P. Walter, Signal integration in the endoplasmic reticulum unfolded protein response, Nat. Rev. Mol. Cell Biol. 8 (7) (2007) 519–529.
[5] L. Qin et al., ER stress negatively regulates AKT/TSC/mTOR pathway to enhance autophagy, Autophagy 6 (2) (2010) 239–247.
[6] E. Szegezdi et al., Mediators of endoplasmic reticulum stress-induced apoptosis, EMBO Rep. 7 (9) (2006) 880–885.
[7] S. Deegan et al., Stress-induced self-cannibalism: on the regulation of autophagy by endoplasmic reticulum stress, Cell. Mol. Life Sci. (2012).
[8] A.M. Gorman et al., Stress management at the ER: regulators of ER stress-induced apoptosis, Pharmacol. Ther. 134 (3) (2012) 306–316.
[9] M.M. Kincaid, A.A. Cooper, ERADicate ER stress or die trying, Antioxid. Redox Signal. 9 (12) (2007) 2373–2387.
[10] R.C. Wek, H.Y. Jiang, T.G. Anthony, Coping with stress: eIF2 kinases and translational control, Biochem. Soc. Trans. 34 (Pt 1) (2006) 7–11.
[11] N. Donnelly et al., The eIF2alpha kinases: their structures and functions, Cell. Mol. Life Sci. 70 (19) (2013) 3493–3511.
[12] L. Moretti et al., Switch between apoptosis and autophagy: radiation-induced endoplasmic reticulum stress?, Cell Cycle 6 (7) (2007) 793–798
[13] B. Levine, Cell biology: autophagy and cancer, Nature 446 (7137) (2007) 745–747.
[14] G. Kroemer, G. Marino, B. Levine, Autophagy and the integrated stress response, Mol. Cell 40 (2) (2010) 280–293.
[15] A. Masud et al., Endoplasmic reticulum stress-induced death of mouse embryonic fibroblasts requires the intrinsic pathway of apoptosis, J. Biol. Chem. 282 (19) (2007) 14132–14139.
[16] S. Gupta et al., Mechanisms of ER stress-mediated mitochondrial membrane permeabilization, Int. J. Cell Biol. (2010).
[17] A. Samali et al., Apoptosis: cell death defined by caspase activation, Cell Death Differ. 6 (6) (1999) 495–496.
[18] R. Hakem et al., Differential requirement for caspase 9 in apoptotic pathways in vivo, Cell 94 (3) (1998) 339–352.
[19] K. Kuida et al., Reduced apoptosis and cytochrome c-mediated caspase activation in mice lacking caspase 9, Cell 94 (3) (1998) 325–337.
[20] S. Gupta et al., HSP72 protects cells from ER stress-induced apoptosis via enhancement of IRE1α-XBP1 signaling through a physical interaction, PLoS Biol. 8 (7) (2010) e1000410.
[21] F. Di Sano et al., Endoplasmic reticulum stress induces apoptosis by an apoptosome-dependent but caspase 12-independent mechanism, J. Biol. Chem. 281 (5) (2006) 2693–2700.
[22] S. Gupta et al., The mitochondrial death pathway: a promising therapeutic target in diseases, J. Cell. Mol. Med. (2009).
[23] M. Boyce et al., A selective inhibitor of eIF2alpha dephosphorylation protects cells from ER stress, Science 307 (5711) (2005) 935–939.
[24] O. Oral et al., Cleavage of Atg3 protein by caspase-8 regulates autophagy during receptor-activated cell death, Apoptosis 17 (8) (2012) 810–820.
[25] E. Wirawan et al., Caspase-mediated cleavage of Beclin-1 inactivates Beclin-1-induced autophagy and enhances apoptosis by promoting the release of proapoptotic factors from mitochondria, Cell Death Dis. 1 (2010) e18.